Journal of Alloys and Compounds 506 (2010) 271–278

Contents lists available at ScienceDirect

Journal of Alloys and Compounds

journal homepage: www.elsevier.com/locate/jallcom

A novel process for producing synthetic rutile and $LiFePO_4$ cathode material from ilmenite

Ling Wu, Xinhai Li*, Zhixing Wang, Huajun Guo, Xiaojuan Wang, Feixiang Wu, Jie Fang, Zhiguo Wang, Lingjun Li

School of Metallurgical Science and Engineering, Central South University, Lushan Street, Changsha 410083, China

ARTICLE INFO

Article history:
Received 22 April 2010
Received in revised form 27 June 2010
Accepted 1 July 2010
Available online 7 July 2010

Keywords:
Ilmenite
Leaching
Synthetic rutile
Cathode material
$LiFePO_4$

ABSTRACT

Synthetic rutile and $LiFePO_4$ cathode materials are prepared from the titanium hydrolysate and iron-rich lixivium, respectively. The titanium hydrolysate and iron-rich lixivium are obtained from the ilmenite by mechanical activation and leaching. The purity of synthetic rutile and the electrochemical performance of $LiFePO_4$ are mainly determined by the leaching process. The optimal leaching conditions are as follows: HCl concentration 20 wt.%, reaction temperature 100 °C and hydrochloric acid/ilmenite mass ratio of 1.2:1. The synthetic rutile prepared under the optimal conditions contains 90.8% TiO_2, 2.21% Fe_2O_3, 0.052% MnO_2 and 0.23% (MgO + CaO), which meet the requirement for the production of titanium dioxide by chlorination. A co-precipitation method is used to synthesize $FePO_4 \cdot xH_2O$ precursor from the iron-rich lixivium. ICP and EDS results show that small amounts of Al and Ti exist in the precursor. XRD results indicate that Al–Ti doping does not obviously change the structure of $LiFePO_4$, and all the $LiFePO_4$ samples are pure triphylite phase. The $LiFePO_4$ sample prepared from the lixivium (leaching with 20 wt.% hydrochloric acid) exhibits a first discharge capacity of 151, 140 and 123 mAh g^{-1} at 1*C*, 2*C* and 5*C* rate, respectively, and shows excellent cycling performance.

1. Introduction

Titanium dioxide, an important intermediate in the manufacture of paints, paper, rubber, ceramics and Li–Ti–O anode materials, is commercially manufactured by two main processes, namely the sulfate process and dry chlorination process. Nowadays, about 60% titanium dioxide is manufactured by the chlorination route in the world [1], in which natural or synthetic rutile is used as raw material. The shortage of natural rutile needs many of efforts to convert ilmenite into synthetic rutile for the chlorination route, and there are several processes for the production of synthetic rutile from ilmenite, such as smelting process [2], Becher process [3], MURSO process [4], ERMS process [5], etc. However, all these processes depend primarily on reductive and/or oxidative thermal pretreatment of ilmenite, which is an extensive energy consuming process. And most of the subsequent acid leaching process requires pressurized conditions, which make the processes complicated and costly. Therefore, developing a simple and economical route is necessary and urgent.

On the other hand, as a promising cathode material for lithium-ion batteries, $LiFePO_4$ is typically prepared from the chemically pure or analytically pure iron salts, such as Fe(II)-oxalate [6–9], Fe(II)-acetate [10], Fe(III)-nitrate [11–14], Fe(II)-sulfate [15–17], Fe(III)-sulfate [18], Fe(II)-chloride [19,20], Fe (III)-citrate [21], Fe_2O_3 [22,23], $FePO_4$ [24], etc. Generally, these highly pure iron salts are prepared from iron-containing ores via complex processes of removing impurities. However, a proper amount of the impurities (Mg, Mn, Al, Ti, etc.) can improve the electrochemical performance of $LiFePO_4$ remarkably, and many researchers also added metallic dopants when they prepared $LiFePO_4$ from highly pure iron salts [8–10,14,15]. Therefore, if we can prepare high-performance cation-substituted $LiFePO_4$ directly from natural ores, a lot of needless reduplicate processes can be avoided and the cost of production would be reduced.

In the present study, we propose a novel and inexpensive process to utilize the natural ilmenite. The major elements of ilmenite, titanium and iron, are utilized to prepare synthetic rutile and the precursor of $LiFePO_4$ cathode material. As a result, almost all the titanium and iron are effectively utilized, and the ultimate products are high value-added.

2. Experimental

The flowsheet of the whole process is shown in Fig. 1. Natural ilmenite from Titanium Company of Panzhihua Steel and Iron Corporation, Sichuan, China, was used as raw material. Its particle size is 50–200 μm, and the chemical composition is listed in Table 1. The ilmenite was mechanically activated by a ball mill before

* Corresponding author. Tel.: +86 731 88836633; fax: +86 731 88836633.
E-mail address: wuling19840404@163.com (X. Li).

0925-8388/$ – see front matter © 2010 Elsevier B.V. All rights reserved.
doi:10.1016/j.jallcom.2010.07.003

Table 1
Chemical composition of the studied ilmenite (wt.%).

TiO_2	FeO	Fe_2O_3	MgO	SiO_2	Al_2O_3	CaO	MnO_2	Total
47.6	32.81	7.25	5.64	3.35	1.66	0.70	0.66	99.67

leaching. The ball mill contains four milling cells, and each cell was 500 ml stainless steel vessel filled with 250 g Ø20 mm, 200 g Ø10 mm and 50 g Ø5 mm steel balls. The milling was operated in air with a rotation speed of 200 rpm and ball/ilmenite mass ratio of 20:1 for 2 h. The activated ilmenite was leached in a 1 L round-bottomed flask attached to a refluxing condenser. First, hydrochloric acid was heated to a designated temperature, and then the ilmenite was added to the solution under vigorous stirring. After various leaching times, the slurry was rapidly cooled and filtered, and then titanium hydrolysate and iron-rich filtrate were obtained. The hydrolysate was washed with 5 wt.% hydrochloric acid, dried at 100 °C, and calcined at 900 °C for 4 h to obtain synthetic rutile.

$LiFePO_4$ cathode material was prepared by using the as-obtained lixivium (filtrate) as starting material. $FePO_4{\cdot}xH_2O$ precursor was synthesized by the following procedures: (1) The lixivium was boiled for 10 min to vaporize the residual HCl, then diluted with deionized water to obtain 0.25 M (Fe) solution; (2) H_3PO_4 (85 wt.%) was added to the solution in a molar ratio of $Fe:PO_4 = 1:1.1$; (3) sufficient concentrated hydrogen peroxide (30 wt.%) was added into the solution to ensure all Fe^{2+} turning to Fe^{3+}; (4) then $NH_3{\cdot}H_2O$ (2 M) was added dropwise into the solution to control the pH at 2.0 ± 0.1, subsequently a cream-colored precipitate formed immediately; (5) after being stirred for 30 min, the precipitate was filtered, washed three times with deionized water and dried in an oven at 80 °C. Thus, $FePO_4{\cdot}xH_2O$ precursor was obtained. Later, Li_2CO_3 and oxalic acid were ball milled with the precursor for 4 h in a molar ratio of $Li:Fe:C = 1:1:1.8$. The obtained mixture was sintered at 600 °C for 12 h under argon atmosphere, followed by natural cooling to room temperature. The $LiFePO_4$ samples prepared from various lixivium (obtained by leaching ilmenite with 15 wt.%, 20 wt.%, 25 wt.% and 30 wt.% hydrochloric acid) were labeled as A, B, C and D, respectively.

The elemental content of samples was analyzed using inductively coupled plasma emission spectroscopy (ICP, IRIS intrepid XSP, Thermo Electron Corporation), and the carbon concentration by C-S analysis (Eltar, Germany). The powder X-ray diffraction (XRD, Rint-2000, Rigaku) using CuKα radiation was employed to identify the crystalline phase of the synthesized material. XRD Rietveld refinement was performed by FULLPROF. The morphology was measured by scanning electron microscope (JEOL, JSM-5600LV) with an accelerating voltage of 20 kV. The elements on the surface of samples were identified by energy-dispersive X-ray spectroscopy (EDS). Conductivity measurements were made on disk-shaped fired samples by four-point D.C. methods.

The electrochemical performance was performed using a two-electrode coin-type cell (CR2025) of $Li|LiPF_6$ (EC:EMC:DMC = 1:1:1 in volume)$|LiFePO_4$. The working cathode is composed of 80 wt.% $LiFePO_4$ powders, 10 wt.% acetylene black as conducting agent, and 10 wt.% poly (vinylidene fluoride) as binder. After being blended in *N*-methyl pyrrolidinone, the mixed slurry was spread uniformly on a thin aluminum foil and dried in vacuum for 12 h at 120 °C. A metal lithium foil was used as anode. Electrodes were punched in the form of 14 mm diameter disks, and the typical positive electrode loadings were in the range of 1.95–2 mg/cm^2. A polypropylene micro-porous film was used as the separator. The assembly of the cells was carried out in a dry argon-filled glove box. The cells were charged and discharged over a voltage range of 2.5–4.1 V versus Li/Li^+ electrode at room temperature.

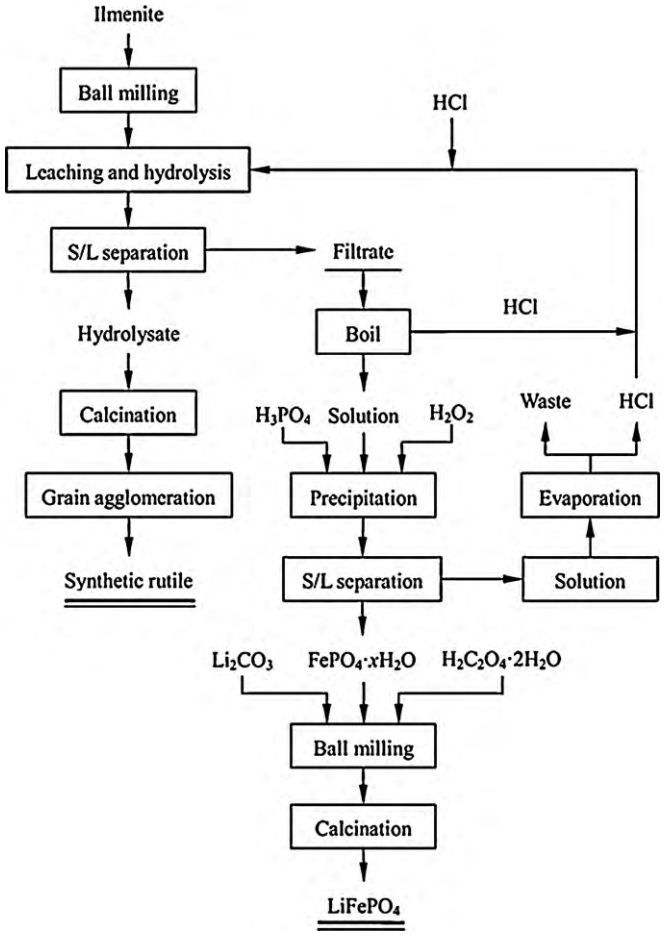

Fig. 1. Schematic flowsheet of the process.

3. Results and discussion

3.1. Leaching process

In order to obtain the high quality synthetic rutile and high-performance $LiFePO_4$, the separation of titanium and iron, and the distribution of impurities (i.e., Mg, Si, Al, Ca and Mn) between the liquid and solid phases are extremely important. In leaching process, the ideal situation is that all of the Fe, Mg, Al, Ca and Mn enter the liquid phase, while Ti and Si are still in the solid phase.

3.1.1. Effect of HCl concentration

Variation of dissolution of Fe and Ti at different hydrochloric acid concentrations with leaching time is shown in Fig. 2. The tests were carried out at 100 °C with the hydrochloric acid/ilmenite mass ratio of 1.2:1. Fig. 2(a) shows that Fe dissolution rate significantly increases with the acid concentration increasing from 15% to 20%, but further increase of acid concentration does not visibly improve the Fe dissolution. On the contrary, the Ti dissolution rate decreases with the increased acid concentration. As shown in Fig. 2(b), Ti dissolution rate under 15% hydrochloric acid is obviously higher than those under 20%, 25% and 30% hydrochloric acid. Furthermore, it can be seen that Fe and Ti dissolution rates show almost no change after 2 h when the concentration of hydrochloric acid is larger than 20%, thus the optimal reaction time 2 h is applied in the subsequent experiments.

Effect of HCl concentration on the elements dissolution was investigated at 100 °C for leaching 2 h, and the results are shown in Fig. 3. It is obvious that Si is not dissolved during the leaching process, even in the 30% HCl concentration. The dissolution rates of Mg, Al, Mn and Ca reach ~99% when the acid concentration increases to 20%, but the elements dissolution rates remain stable with further increase of the acid concentration.

The obtained titanium hydrolysate was calcined at 900 °C for 4 h to prepare rutile. The chemical composition of the prepared rutile is listed in Table 2. It can be seen that the TiO_2 content rapidly increases from 70.4% to 90.8% with the acid concentration increasing from 15% to 20%, which accompanies the sharp decrease of Fe_2O_3 content from 19.5% to 2.21%. However, the TiO_2 content gradually increase and Fe_2O_3 content gradually decrease when further increase the acid concentration. The results are in good agreement with that we discussed in Figs. 2 and 3. Therefore, the expected leaching results can be achieved with 20–30% HCl concentration.

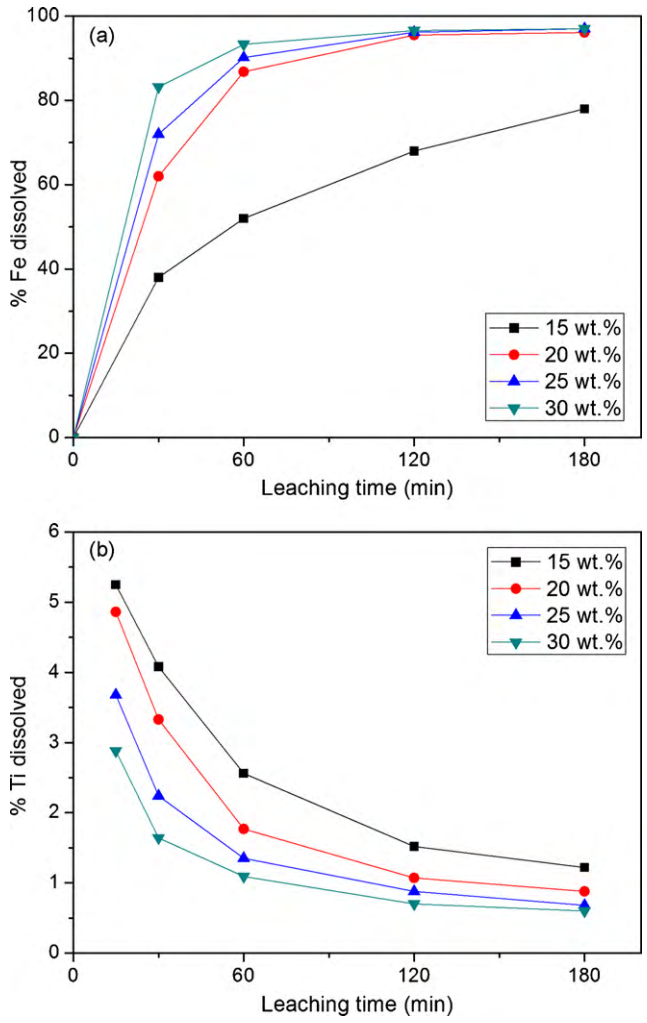

Fig. 2. Effect of hydrochloric acid concentration on Fe (a) and Ti (b) dissolution.

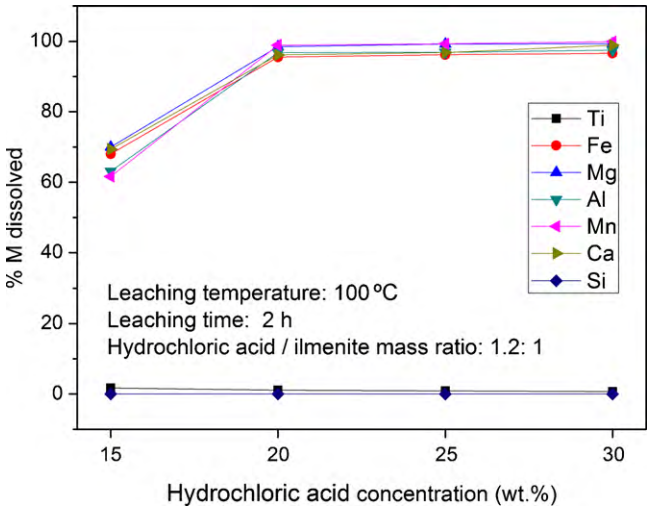

Fig. 3. Effect of hydrochloric acid concentration on the elements dissolution.

Table 2
Effect of hydrochloric acid concentration on preparation of synthetic rutile.

Hydrochloric acid concentration (wt.%)	Fe_2O_3 in rutile (wt.%)	TiO_2 in rutile (wt.%)	TiO_2 losses in solution (%)
15	19.50	70.4	1.72
20	2.21	90.8	1.07
25	1.78	91.3	0.88
30	1.55	92.0	0.70

Hydrochloric acid/ilmenite mass ratio: 1.2:1, temperature: 100 °C, leaching time: 2 h.

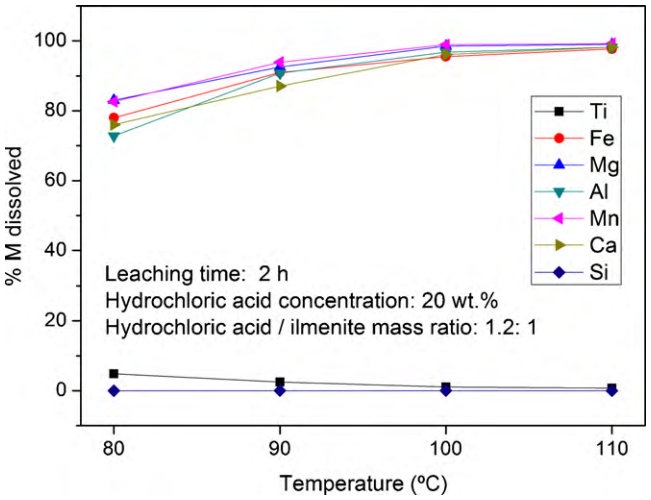

Fig. 4. Effect of reaction temperature on the elements dissolution.

Nevertheless, in order to reduce the volatility of HCl and recycle the hydrochloric acid, 20% acid concentration is selected as the optimal condition.

3.1.2. *Effect of reaction temperature*

Fig. 4 shows the results of experiments carried out with 20 wt.% hydrochloric acid and acid/ilmenite mass ratio of 1.2:1. When the temperature is below 100 °C, the dissolution rates of Fe, Mg, Al, Mn and Ca significantly increase with the temperature, but the Ti dissolution decreases with the temperature. The Fe, Mg, Al, Mn and Ca dissolution rates 78%, 83%, 72.8%, 82.6% and 76% sharply increase to 97.7%, 99%, 98.2%, 99.2% and 98.2% when the temperature increases from 80 to 100 °C. This is accompanied with the decrease of Ti dissolution from 4.83% to 1.07%. The hydrolysis reaction of $TiOCl_2$ is known to be much enhanced at higher temperature, which is thought to be the main reason for the improvement in the impurity elements removal and Ti recovery. However, further raising the temperature to 110 °C does not yield obvious changes of all the elements dissolution.

Chemical analysis of the synthetic rutile prepared at different temperatures is listed in Table 3. The TiO_2 and Fe_2O_3 contents of rutile show significant changes by increasing the reaction temperature from 80 to 100 °C, and little change from 100 to 110 °C, which

Table 3
Effect of reaction temperature on preparation of synthetic rutile.

Reaction temperature (°C)	Fe_2O_3 in rutile (wt.%)	TiO_2 in rutile (wt.%)	TiO_2 losses in solution (%)
80	15.80	74.7	4.83
90	7.46	85.6	2.47
100	2.21	90.8	1.07
110	1.46	91.6	0.72

Hydrochloric acid concentration: 20 wt.%, hydrochloric acid/ilmenite mass ratio: 1.2:1, leaching time: 2 h.

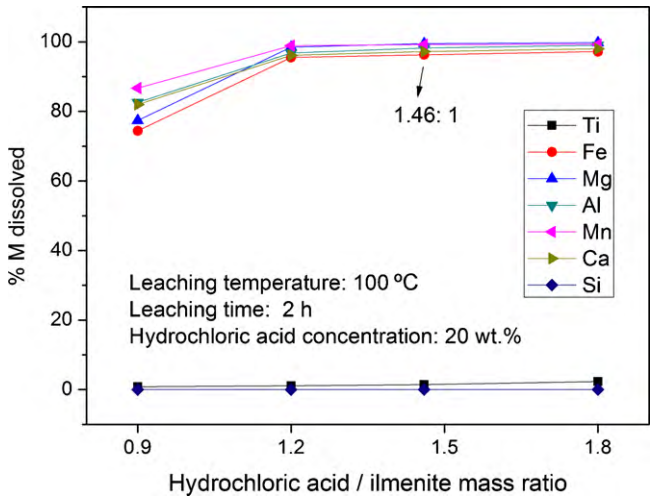

Fig. 5. Effect of hydrochloric acid/ilmenite ratio on the elements dissolution.

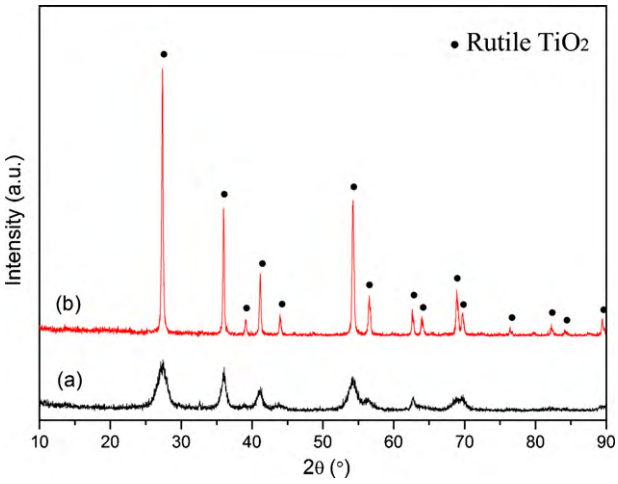

Fig. 6. XRD patterns of the titanium hydrolysate (a) and synthetic rutile (b) prepared under the optimal conditions.

is consistent with the results in Fig. 4. Thus, the optimal reaction temperature is 100 °C.

3.1.3. *Effect of hydrochloric acid/ilmenite ratio*

The effect of hydrochloric acid (100% HCl)/ilmenite mass ratio on elements dissolution (Fig. 5) was studied at 100 °C with 20 wt.% hydrochloric acid. The acid/ilmenite mass ratios range from 0.9:1 to 1.8:1. The theoretic acid consumption (acid/ilmenite mass ratio of 1.46:1) was calculated with the reaction formulas (1) and (2).

$$FeO{\cdot}TiO_2 + 4HCl = FeCl_2 + TiOCl_2 + 2H_2O \quad (1)$$

$$Fe_2O_3 + 6HCl = 2FeCl_3 + 3H_2O \quad (2)$$

Fig. 5 shows that the Fe, Mg, Al, Mn and Ca dissolution rates obviously increase with the acid/ilmenite mass ratio increasing from 0.9:1 to 1.2:1, and then tend to be constant at higher ratios. The Ti losses in solution increases from 0.85% to 2.32% with acid/ilmenite mass ratio increasing from 0.9:1 to 1.8:1, due to the high acid/solid ratio greatly inhibits the titanium hydrolysis and precipitation.

The chemical composition of the prepared rutile is listed in Table 4. It is found that the purity of rutile increases with the hydrochloric acid/ilmenite ratio, and the high quality rutile (>90%) can be obtained when the ratio is larger than 1.2:1. Considering the quality of rutile, the losses of titanium in solution and the acid consumption, the optimum acid/ilmenite mass ratio is 1.2:1.

3.2. *Synthetic rutile*

Fig. 6 shows the XRD patterns of the titanium hydrolysate and synthetic rutile prepared under the optimal conditions. The XRD pattern of hydrolysate displays the diffraction peaks of rutile, which indicates that the rutile phase begins to form during the coupled dissolution and hydrolysis process. However, all the peaks are weak and broad, indicating low crystallinity. The hydrolysate was calcined at 900 °C for 4 h to obtain crystalline TiO_2. Its XRD pattern matches both the Bragg-position and intensity of rutile (JCPDS no. 71-0650), which demonstrates that a synthetic rutile with high crystallinity was prepared.

Fig. 7(a) and (b) shows the SEM image and EDS of the synthetic rutile prepared under the optimal conditions, respectively.

Table 4
Effect of hydrochloric acid/ilmenite ratio on preparation of synthetic rutile.

Hydrochloric acid/ilmenite mass ratio	Fe_2O_3 in rutile (wt.%)	TiO_2 in rutile (wt.%)	TiO_2 losses in solution (%)
0.9:1	16.86	73.2	0.85
1.2:1	2.21	90.8	1.07
1.46:1	1.56	91.6	1.47
1.8:1	1.15	92.9	2.32

Hydrochloric acid concentration: 20 wt.%, temperature: 100 °C, leaching time: 2 h.

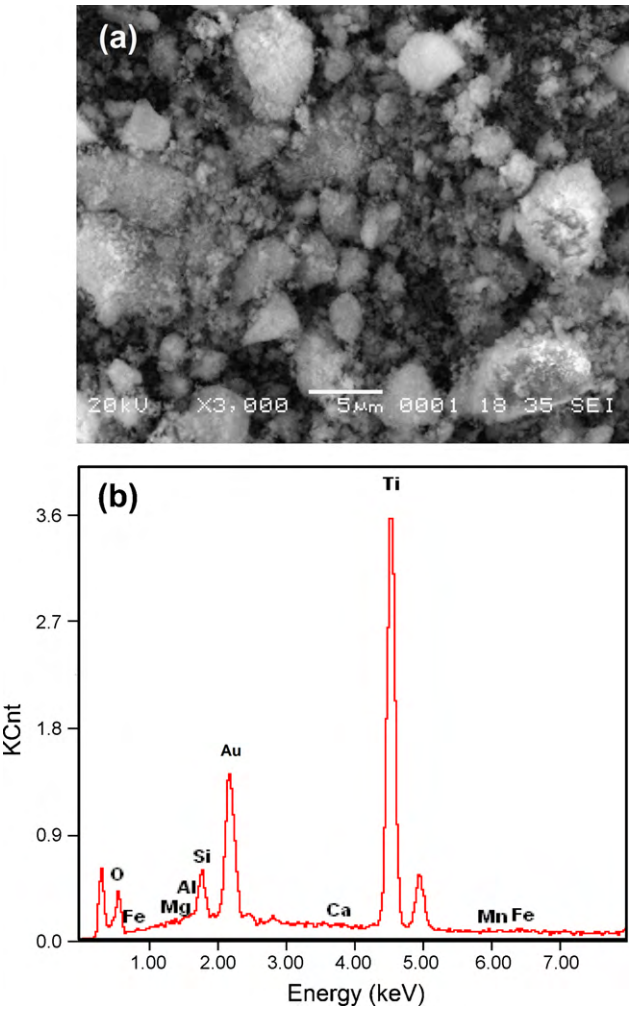

Fig. 7. SEM image (a) and EDS (b) of the synthetic rutile prepared under the optimal conditions.

Table 5
Chemical composition (wt.%) of the synthetic rutile prepared under the optimal conditions.

TiO_2	Fe_2O_3	MgO	Al_2O_3	MnO_2	CaO	SiO_2
90.8	2.21	0.106	0.105	0.052	0.124	6.421

Table 6
Chemical composition of the starting material (the lixivium leached by 20 wt.% hydrochloric acid), pK_{sp} (25 °C) and theoretic initial precipitation pH (pH_0) of the corresponding insoluble compounds.

Elements	Fe	Mg	Mn	Al	Ca	Ti	Si
Concentration (mol/L)	0.25	0.0680	0.0038	0.0147	0.0056	0.0027	~0
Insoluble compounds pK_{sp}	21.89	23–27	12	18.24	28.7	29	–
Precipitation pH_0	0.318	3.496–4.163	4.219	0.728	3.755	0.784	–

Table 7
The molar ratio of Li, Fe, P, Mg, Mn, Al, Ca and Ti in $LiFePO_4$ samples.

Samples	Li	Fe	P	Mg	Mn	Al	Ca	Ti
A	0.905	0.981	1	0	0	0.0160	0	0.0212
B	0.947	0.980	1	0	0	0.0166	0	0.0109
C	0.961	0.986	1	0	0	0.0166	0	0.0076
D	0.966	0.984	1	0	0	0.0168	0	0.0053

As shown, the sample exhibits nano-scale primary particles, and the primary particles agglomerate to secondary particles in the size of 2–8 μm. The grain size is finer than the required specification for the titanium dioxide chlorination process (>50 μm) [25]. Thus, an additional granulation process is needed to increase the particle size. From EDS pattern (Fig. 7(b)), it can be seen that the sample contains major elements Ti, O, Si and trace elements Fe, Mn, Ca, Al and Mg. Further, the accurate chemical composition of the sample is determined by ICP, and the results are listed in Table 5. As shown, the contents of MgO, MnO_2 and CaO are low enough to meet the requirement for the production of titanium dioxide by chlorination process. The Fe_2O_3 content is slightly higher than the standard value (≤1.5%), which is generally accepted in industry, and it could be reduced by prolonging the leaching time or increasing the acid/ilmenite ratio.

3.3. *$LiFePO_4$ cathode material*

As the starting material, the lixivium was firstly diluted with deionized water to obtain 0.25 M (Fe) solution. The elemental concentration of starting material (the lixivium leached by 20 wt.% hydrochloric acid), pK_{sp} (25 °C) and theoretic initial precipitation pH (pH_0) of the insoluble compounds ($FePO_4$, $Mg_3(PO_4)_2$, $MnNH_4PO_4$, $AlPO_4$, $Ca_3(PO_4)_2$ and $TiO(OH)_2$) are listed in Table 6. The pH_0 is calculated with the elemental concentration and pK_{sp}, according to the solid solubility formula [26]. It is found that the initial precipitation pH values of Fe, Mg, Mn, Al, Ca and Ti are 0.318, 3.496, 4.219, 0.728, 3.755 and 0.784, respectively. The results indicate that Al and Ti could enter the $FePO_4{\cdot}xH_2O$ precursor under the reaction pH value 2.0, while, other elements, Mg, Mn and Ca will be totally excluded from the precursor in theory.

Table 7 shows the chemical composition of $LiFePO_4$ samples. The samples prepared from various lixivium (obtained by leaching ilmenite with 15 wt.%, 20 wt.%, 25 wt.% and 30 wt.% hydrochloric acid) are labeled as A, B, C and D, respectively. As shown, a small amount of Al and Ti are detected in all the samples, whereas Mg, Mn and Ca are not detected. The experimental results are in good agreement with what we expected in Table 6. The Ti content decreases from samples A to D, which is ascribed to that the Ti losses in lixivium decreases with the increased HCl concentration. However, Al content remains stable, owing to the similar Al/Fe ratios of all the lixivium.

The XRD patterns of $LiFePO_4$ samples are shown in Fig. 8. As shown, the diffraction lines of all samples are indexed to an orthorhombic crystal structure (triphylite, space group *Pnma*), and no impurity phases are detected. C-S analysis confirms that the remaining carbon of samples A, B, C and D is 1.12 wt.%, 0.89 wt.%, 0.84 wt.% and 0.93 wt.%, respectively. The carbon comes from the oxalic acid during annealing procedure. Nevertheless, no diffraction peaks of carbon are detected, indicating that it is amorphous. It is found that Al–Ti doping does not obviously change the structural characteristics of $LiFePO_4$. However, the intensity of XRD peaks decreases with the increased dopants amounts (i.e., from D to A), which reveals that Al^{3+} and Ti^{4+} ions have entered the lattices of $LiFePO_4$ crystal.

Previous studies have shown that metallic ions could occupy Li site (M1), Fe site (M2) or both [8–10,27,28]. In order to clarify whether the dopants occupy Li site or Fe site, the atom positions

Table 8
Results of structural analysis obtained from X-ray Rietveld refinement of $LiFePO_4$ sample B.

Atoms	Site	*x*	*y*	*z*	Occupancy
Li	4a	0	0	0	0.9536(7)
Al	4a	0	0	0	0.0020(9)
Ti	4a	0	0	0	0.0101(10)
Fe	4c	0.2824(8)	0.25	0.9740(9)	0.9787(9)
Al	4c	0.2824(8)	0.25	0.9740 (9)	0.0142(11)
P	4c	0.0952(6)	0.25	0.4183(5)	1
O1	4c	0.0964(10)	0.25	0.7420(6)	1
O2	4c	0.4560(7)	0.25	0.2055(9)	1
O3	8d	0.1647(9)	0.0482(9)	0.2836(8)	1

Space group: *Pnma*. R_p = 7.84%, R_{wp} = 9.71%, R_{exp} = 5.48%.
Cell constant (Å): *a* = 10.3262(8), *b* = 6.0087(6), *c* = 4.6998(9); cell volume (Å^3): 291.6087(9).

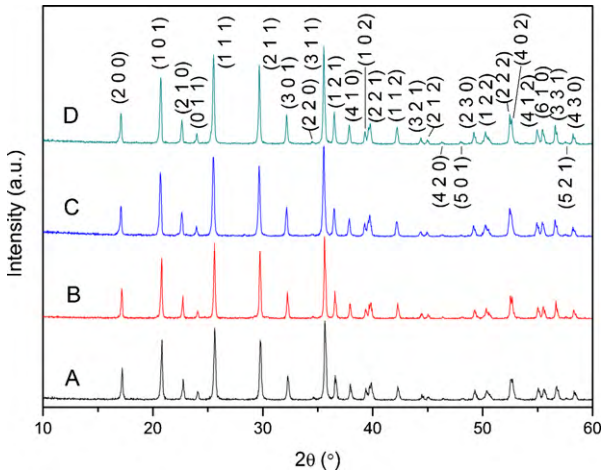

Fig. 8. XRD patterns of $LiFePO_4$ samples synthesized from various lixivium.

and occupancy were refined by Rietveld method. We attempted all the possible occupying ways, and the best refinement result was only obtained when constrained Ti^{4+} to occupy M1 site and Al^{3+} to occupy both sites. As a typical case, the Rietveld-refined X-ray diffraction pattern of sample B is shown in Fig. 9, and the crystal parameters are summarized in Table 8. As shown, the observed and calculated patterns match well. It is found that Ti^{4+} ions and partial Al^{3+} ions substitute on M1 site with charge compensating vacancies (Li vacancies) on M1 site, and partial Al^{3+} ions substitute on M2 site with charge compensating vacancies (Fe vacancies) on M2 site. It is also noted that the calculated atomic ratio of Li, Fe, Al, Ti and P (Table 8, occupancy), 0.9536:0.9787:(0.0020 + 0.0142):0.0101:1, is basically consistent with the ICP result (Table 7, sample B), 0.947:0.980:0.0166:0.0109:1. Furthermore, we also refined the XRD data of samples A, C and D, and similar results were obtained.

SEM images show that all the $LiFePO_4$ samples exhibit similar morphologies. As a typical case, Fig. 10(a) and (b) shows the SEM image and corresponding EDS pattern of sample B, respectively. As shown, fine particles in the size of 0.1–1 μm can be observed. The EDS result indicates that the sample contains a small amount of Al and Ti, but does not contain Mg, Ca, Mn and Si, which is consistent with the ICP results in Table 7.

Fig. 11 displays the initial charge/discharge curves of $LiFePO_4$ samples at various *C* rates. As shown, all the samples exhibit good electrochemical properties. The samples A, B, C and D show initial

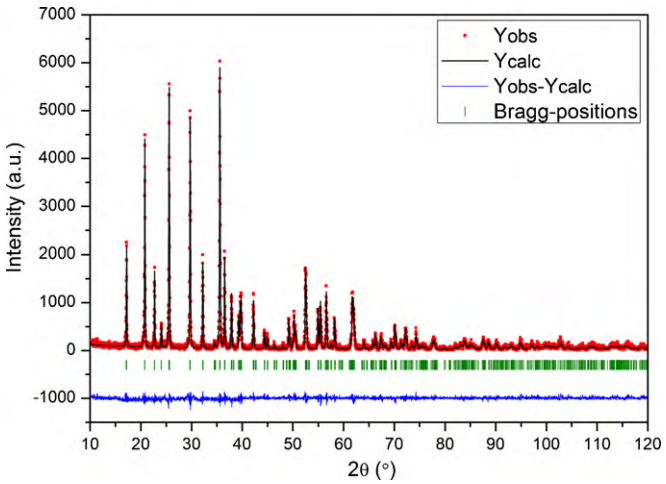

Fig. 9. Rietveld-refined X-ray diffraction pattern of $LiFePO_4$ sample B.

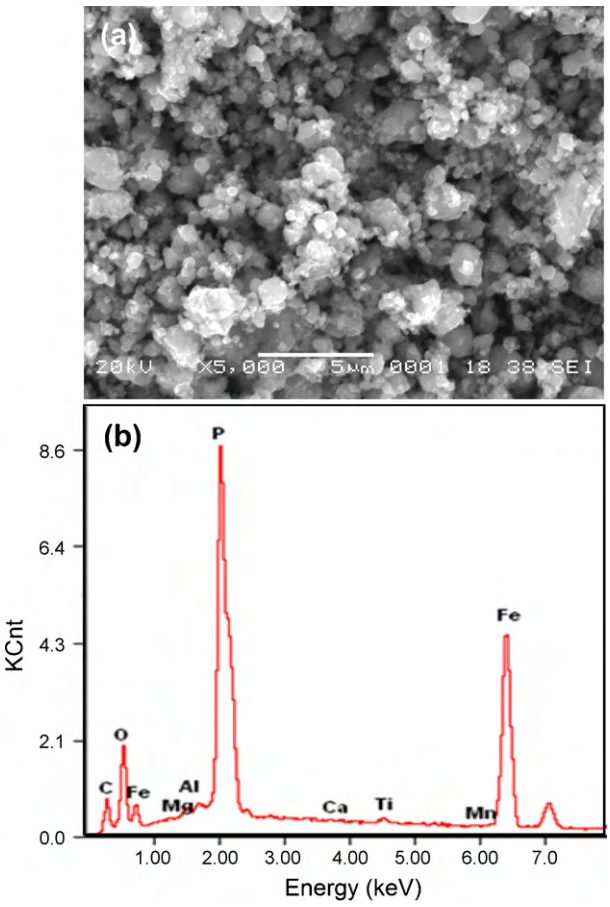

Fig. 10. SEM image (a) and EDS pattern (b) of $LiFePO_4$ sample B.

discharge capacity of 152, 159, 162 and 163 mAh g^{-1} at 0.1*C* rate, and 144, 151, 153 and 154 mAh g^{-1} at 1*C* rate, respectively. The capacity at low current densities decreases from samples D to A, owing to the increased impurity content (Al^{3+} and Ti^{4+}). By increasing the current density, the utilization rate of the active materials decreases along with the polarization of electrodes increases. Samples A, B, C and D exhibit a capacity of 135, 140, 141 and 141 mAh g^{-1} at 2*C* rate, and 119, 123, 120 and 116 mAh g^{-1} at 5*C* rate, respectively. At higher current densities, the polarization of electrodes increases from samples A to D, which should be ascribed to the conductivity of $LiFePO_4$ decrease with the reduced doping amount. The electrical conductivity of samples A, B, C and D is 1.12×10^{-2}, 1.09×10^{-2}, 9.95×10^{-3} and 9.92×10^{-3} S cm^{-1}, respectively.

Cycling performance of $LiFePO_4$ samples is shown in Fig. 12. It is found that all the samples show about 100% capacity retention after 100 cycles at 1*C* and 2*C* rates. But at higher current rate (5*C*), the capacity retention of A, B, C and D at 100th cycle is reduced to 96.6%, 95.9%, 93.3% and 93.1%, respectively. However, the capacity retention of all the samples is still higher than 93%.

The excellent electrochemical properties of the final products confirm that synthesis high-performance $LiFePO_4$ from ilmenite lixivium is practicable. The performance of $LiFePO_4$ is related to the Al and Ti content of lixivium, whereas is irrelevant to the content of Mg, Mn and Ca. Because the Al content of natural ilmenite is usually very low, thus, the key step is to control the Ti content of lixivium. Therefore, the Ti losses in the lixivium must be controlled to a relatively low value by optimizing leaching process.

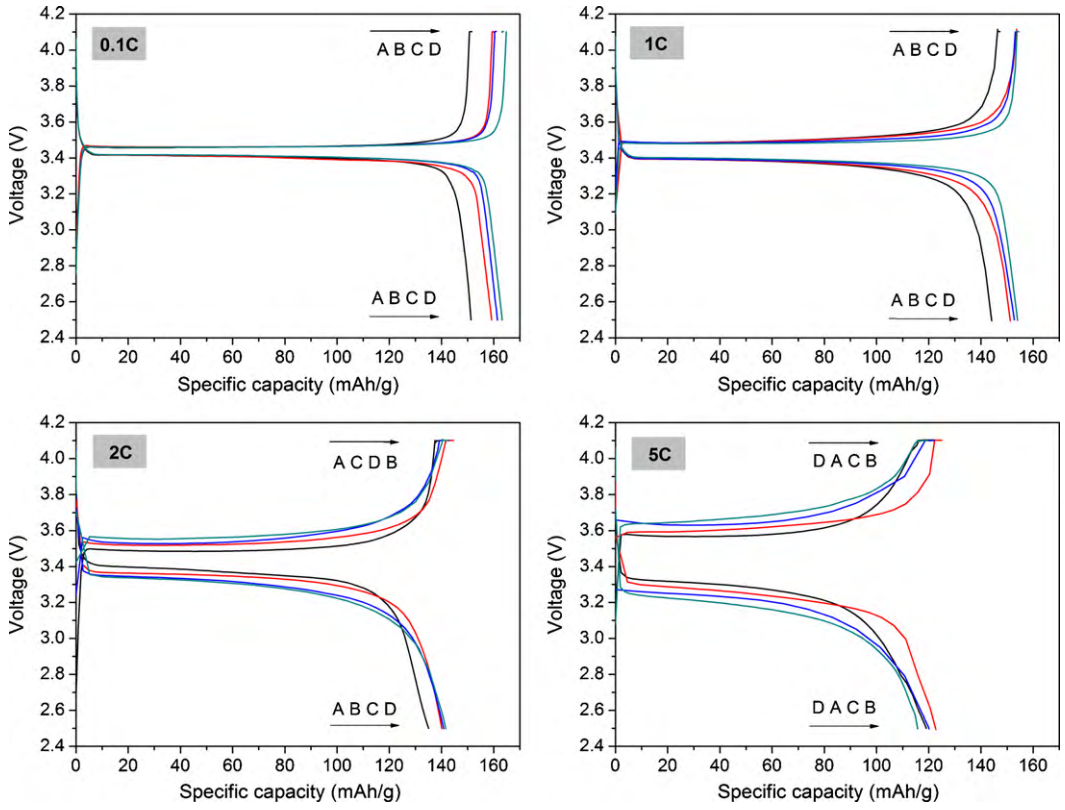

Fig. 11. The initial charge and discharge curves of $LiFePO_4$ samples at various *C* rates.

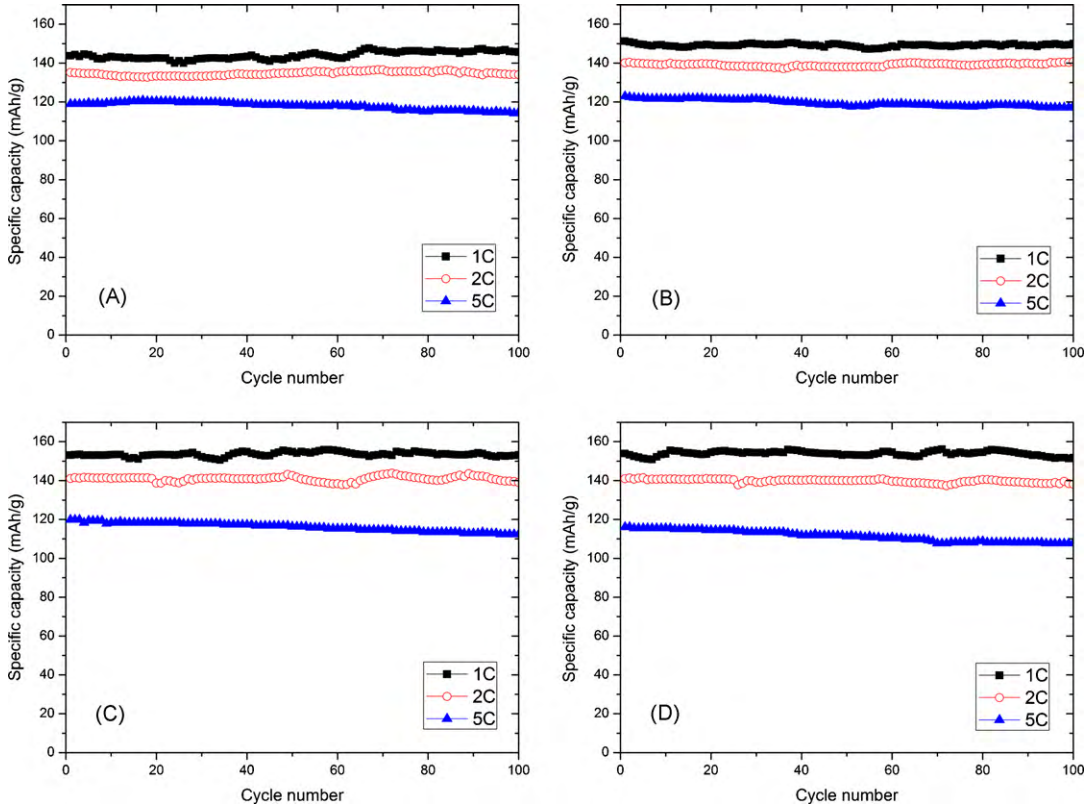

Fig. 12. Cycling performance of $LiFePO_4$ samples at various *C* rates.

4. Conclusions

High quality synthetic rutile and high-performance $LiFePO_4$ cathode material are successfully prepared from the natural ilmenite. The quality of synthetic rutile and the performance of $LiFePO_4$ are largely determined by the leaching process. The optimal leaching conditions are as follows: HCl concentration 20 wt.%, reaction temperature 100 °C and hydrochloric acid/ilmenite mass ratio of 1.2:1. Under the optimal conditions, almost all of the Fe, Mg, Al, Ca and Mn would enter the liquid phase, whereas Ti and Si remain in the slag, and the obtained synthetic rutile meets the requirement for the production of titanium dioxide by chlorination. $LiFePO_4$ cathode materials are prepared from various lixivium. It is found that all the $LiFePO_4$ samples show excellent electrochemical properties. In this work, three goals can be achieved, namely the utilization of ilmenite, preparation of high quality synthetic rutile and synthesis of high-performance $LiFePO_4$. In a word, almost all of the titanium and iron are effectively utilized and the ultimate products are high value-added. Based on these results, we believe that this method is a promising process to comprehensively utilize the natural ilmenite.

Acknowledgement

This project was sponsored by the National Basic Research Program of China (973 Program, 2007CB613607).

References

[1] C. Li, B. Liang, L.-H. Guo, Hydrometallurgy 89 (2007) 1.
[2] R.H. Natziger, G.W. Elger, US Bureau of Mines, Report Invest No. 9065, 1987.
[3] R.G. Becher, Australian Patent 247110, 1963.
[4] H.N. Sinha, Proceedings of the Eleventh Commonwealth Mining and Metallurgical Congress, Institute of Mining and Metallurgy, London, 1979, p. 669.
[5] E.A. Walpole, Heavy Minerals, SAIMM, Johannesburg, 1997, p. 169.
[6] K. Zaghib, N. Ravet, M. Gauthier, F. Gendron, A. Mauger, J.B. Goodenough, C.M. Julien, J. Power Sources 163 (2006) 560.
[7] H.C. Shin, S.B. Park, H. Jang, K.Y. Chung, W.I. Cho, C.S. Kim, B.W. Cho, Electrochim. Acta 53 (2008) 7946.
[8] N. Meethong, Y.-H. Kao, S.A. Speakman, Y.-M. Chiang, Adv. Funct. Mater. 19 (2009) 1060.
[9] S.-Y. Chung, J.T. Bloking, Y.-M. Chiang, Nat. Mater. 1 (2002) 123.
[10] Y. Hu, M.M. Doeff, R. Kostecki, R. Finones, J. Electrochem. Soc. 151 (2004) A1279.
[11] H. Liu, J. Xie, K. Wang, Solid State Ionics 179 (2008) 1768.
[12] Z.-R. Chang, H.-J. Lv, H.-W. Tang, H.-J. Li, X.-Z. Yuan, H. Wang, Electrochim. Acta 54 (2009) 4595.
[13] B. Wang, Y. Qiu, L. Yang, Electrochem. Commun. 8 (2006) 1801.
[14] J. Ying, M. Lei, C. Jiang, C. Wan, X. He, J. Li, L. Wang, J. Ren, J. Power Sources 158 (2006) 543.
[15] J.F. Ni, H.H. Zhou, J.T. Chen, X.X. Zhang, Mater. Lett. 59 (2005) 2361.
[16] D. Jugovic, M. Mitric, N. Cvjeticanin, B. Jancar, S. Mentus, D. Uskokovic, Solid State Ionics 179 (2008) 415.
[17] Z. Wang, S. Su, C. Yu, Y. Chen, D. Xia, J. Power Sources 184 (2008) 633.
[18] R. Yang, X. Song, M. Zhao, F. Wang, J. Alloys Compd. 468 (2009) 365.
[19] M. Konarova, I. Taniguchi, Mater. Res. Bull. 43 (2008) 3305.
[20] M. Konarova, I. Taniguchi, Powder Technol. 191 (2009) 111.
[21] Y. Cui, X. Zhao, R. Guo, J. Alloys Compd. 490 (2010) 23.
[22] H.-P. Liu, Z.-X. Wang, X.-H. Li, H.-J. Guo, W.-J. Peng, Y.-H. Zhang, Q.-Y. Hu, J. Power Sources 184 (2008) 469.
[23] M.E. Zhong, Z.T. Zhou, Mater. Chem. Phys. 119 (2010) 428.
[24] Y. Wang, J. Wang, J. Yang, Y. Nuli, Adv. Funct. Mater. 16 (2006) 2135.
[25] M.H.H. Mahmoud, A.A.I. Afifi, I.A. Ibrahim, Hydrometallurgy 73 (2004) 99.
[26] H. Stephen, T. Stephen, Solubilities of Inorganic Compounds, vol. 1, Pergamon Press, Oxford, 1963.
[27] L. Wu, X.-H. Li, Z.-X. Wang, L.-J. Li, J.-C. Zheng, H.-J. Guo, Q.-Y. Hu, J. Fang, J. Power Sources 189 (2009) 681.
[28] R. Amin, C. Lin, J. Maier, Phys. Chem. Chem. Phys. 10 (2008) 3519.